Behavior of Pozzolanic Pavements Under Load

ERNEST J. BARENBERG, Assistant Professor, Department of Civil Engineering, University of Illinois

Cured and hardened pozzolanic materials are strong and resistant to flexing, thus distributing the load over a large area by slab action. This report presents the results of a study of the behavior of pozzolanic pavements under static and dynamic loads. Load-deflection characteristics and the ultimate load-carrying capacity of the slabs under static loads are discussed in terms of elastic and ultimate theory. The behavior of pozzolanic test pavements under repeated loads is compared with fatigue data from flexure specimens, and criteria for predicting the fatigue life of the pavements are discussed.

•POZZOLANIC MATERIALS are rapidly assuming a role of economic significance in many areas of the country. The availability of suitable quality fly ash in these areas enables the lime-fly ash aggregate to be used competitively with other stabilized materials as a quality paving material. The outstanding performance of many miles of pozzolanic pavements now in service is a testimony to the durability of the material.

Since pozzolanic materials require an asphaltic wearing surface for best performance, there is a tendency to classify pozzolanic pavements as flexible pavements, and to base the thickness design on the same factors which influence the thickness design of unbound granular materials. These materials, however, develop considerable flexural rigidity, and thus a pozzolonic pavement behaves more nearly like a rigid pavement than a flexible one. A research program was undertaken to demonstrate the slab-type behavior of pozzolanic pavements under static and dynamic loads. Significant findings from this program are reported herein.

The research program on the behavior of pozzolanic pavements was a part of a larger program on pozzolanic materials conducted at the University of Illinois, but only the results pertinent to the behavior of pozzolanic pavements are discussed in this paper. The results from other phases of the program have either been reported (1, 2) or will be presented in technical publications in the near future.

TEST PROGRAM

Research on pozzolanic materials and pavements was divided into two parts: a laboratory investigation to evaluate the physical properties of the material, and a pavement behavior and evaluation phase. The laboratory program was conducted before initiating the pavement behavior phase to guide the research staff in the selection of the pavement characteristics to be studied. Pavement behavior observation and evaluation were carried out at the University of Illinois pavement test track, and consisted of both static and dynamic tests on the pavement. The test track facilities and its capabilities are discussed by Ahlberg and Barenberg (1).

In the laboratory phase of the program, fundamental studies were carried out to determine the physical properties of the pozzolanic material including strength, change in strength with time, modulus of elasticity, Poisson's ratio, fatigue properties and resistance to alternate cycles of freezing and thawing and wetting and drying.

Paper sponsored by Committee on Rigid Pavement Design.

TABLE 1

SCHEDULE OF POZZOLANIC PAVEMENTS TESTED

Test Pavement	Thickness	Flexural Strength[a] (psi)	Type Load
(a) Test Set I			
1	4.0	98	Static-interior
2	4.0	104	Static-interior
3	4.0	275	Static-interior
4	4.0	280	Static-interior
5	4.0	287	Static-edge
6	4.0	290	Static-edge
7	4.0	79	Static-interior
8	4.0	86	Static-interior
(b) Test Set II			
1	4.3	185	Dynamic-interior
2	3.8	185	Dynamic-interior
4	4.8	185	Dynamic-interior
5	4.3	185	Dynamic-interior
(c) Test Set III			
1	4.3	75	Dynamic-interior
2	4.8	75	Dynamic-interior
3	5.3	75	Dynamic-interior
4	5.8	75	Dynamic-interior
5	4.8	75	Dynamic-interior
6	5.3	75	Dynamic-interior
(d) Test Set IV			
1	4.0	76	Dynamic-edge
2	4.0	170	Dynamic-edge
3	4.0	230	Dynamic-edge
4	5.5	230	Dynamic-edge
5	5.5	170	Dynamic-edge
6	5.5	76	Dynamic-edge

[a]At initial loading.

TABLE 2

PHYSICAL CHARACTERISTICS OF SUBGRADE MATERIAL

Characteristic	AASHO Designation	Value
AASHO class.		A-6 (8)
Opt. moist. cont.	T99-57	13.0
Max. dry dens.	T99-57	120
L. L., %	T89-54	25
P. L., %	T90-54	14
P. I., %	T91-54	11
Grain-size distr, % passing sieve:	T88-57	
No. 4		98
No. 10		96
No. 40		92
No. 100		85
No. 200		79
0.02 mm		61
0.05 mm		39
0.002 mm		27

In the pavement behavior and evaluation phase of the program, 8 pavement sections were tested to failure under static loads positioned at the interior and near the edge of the pavement. In addition, 34 pavement sections were tested under dynamic loads; 18 were standard flexible pavements with crushed stone bases and various surfaces and 16 were pozzolanic pavements. The thickness, strength, and position of the loads were altered for the different test pavements.

Only the test results from the pozzolanic pavements are presented in this paper. A summary of these pavements is given in Table 1. Test pavements 3 and 6 of test set II were made of crushed stone base and so were omitted from the table.

Materials and Construction Procedures

The properties of the materials used in the pavement behavior and evaluation phase of the program as reported by Ahlberg and Barenberg (1) are repeated here for reference.

Subgrade. — One hundred and fifty tons of selected subgrade material was taken from borrow pit No. 1 for the AASHO Road Test near Ottawa, Ill. Routine classification tests were made in the laboratory on samples of the subgrade material, which was a yellow-brown soil with an AASHO classification of A-6. The physical characteristics of the subgrade soil are summarized in Table 2. Additional information on soil from the same source is available in publications (5, 6) relating to the AASHO Road Test.

Before placing the subgrade soil, a granular filter was placed on the bottom of the test track pit. The filter material was a graded aggregate ranging from 3/4-in. to minus No. 200 sieve. The granular filter was compacted with a pneumatic tamper.

After the granular filter had been placed and compacted, the subgrade was placed over the filter material. Before placing the soil in the test track pit, vertical sheet metal separators were placed along both the interior and external walls of the test track pit so that the subgrade soil and the material for the vertical granular filter could be kept separate. The soil and the filter material were maintained at approximately the same level during placing. The filter material and

TABLE 3

COMPACTED PROPERTIES OF THE SUBGRADE

Property	Test Set			
	I	II	III	IV
Compacted density, pcf	91.9	117.6	116.6	115.1
Percent of standard	76.7	98.0	97.2	95.9
Moisture content, %	15.7	13.1	12.8	13.6
Modulus of subgrade reaction, psi/in.	50.0	150.0	163.0	60.0

TABLE 4

GRADATION OF GRAVEL FOR POZZOLANIC BASE

Sieve Size	Grain Size Distr.[a] (%)
3/4-in.[b]	100
3/8-in.	87
No. 4	73
No. 10	52
No. 40	23
No. 200	8
0.02 mm	4
0.05 mm	2
0.002 mm	1

[a]AASHO designation, T88-57.
[b]Material larger than 3/4 in. discarded.

TABLE 5

PROPERTIES OF FLY ASH FOR POZZOLANIC BASE

Property	Value (%)
Major constituent (approx.):	
Silicon dioxide	41
Aluminum oxide	25
Ferric oxide	21
Calcium oxide	4
Sulfur trioxide	1
Loss on ignition	7.2
Grain-size distr., passing sieve:	
No. 10	100
No. 40	98
No. 200	87
No. 325	79

the subgrade soil were first compacted around the vertical separators by hand. The vertical separators were removed before final compaction.

The subgrade soil was placed in the track and pulverized with a rotary hoe. Water was added to the soil during pulverization to bring the soil to the desired moisture content. The material was compacted in layers with 3-in. compacted thickness. Several methods of compaction were investigated to determine which would give the most uniform results. After considerable experimentation, it was found that, of the methods tried, pneumatic tampers gave the most uniform densities. Three to five passes of the tampers were required to bring the soil to the desired density. Alternate passes of the tamper were made in transverse directions to minimize directional densification of the subgrade.

During the process of subgrade placement, continuous testing was performed to control the moisture content and compacted density. After the soil was placed and brought to grade, plate-bearing tests were conducted on the subgrade. Results are given in Table 3. In-place CBR tests were performed on most subgrades with the CBR values for the subgrade soil of test sets II and III between 15 and 20, and for test sets I and IV between 2 and 5. For test sets I and IV the subgrade soil was intentionally placed wet of optimum to obtain the desired low CBR and plate-bearing values.

At the completion of each test set, the subgrade material was removed to a depth of 1 ft or more, pulverized, and replaced in the manner previously described before placing the base courses for the next test set.

A special soil planer was developed to bring the subgrade to the desired elevation. The planer trimmed the subgrade to a tolerance of ± 0.03 in., and the compacted base materials to within ± 0.1 in.

Pozzolanic Bases. — The pozzolanic material used in this study was composed of 82 percent gravel, 14 percent fly ash, and 4 percent lime. The gravel used for the pozzolanic bases came from a stockpile of subbase material used in the AASHO Road Test, and was the same material as was used for the cement-treated and bituminous-treated bases in the special base study of the AASHO Test (5). The grain-size distribution of the gravel is given in

TABLE 6

PROPERTIES OF LIME FOR POZZOLANIC BASE

Property	Value (%)
Major constituents (approx.):	
Calcium carbonate	4
Calcium hydroxide	59
Magnesium hydroxide	2
Magnesium oxide	33
Grain-size distr., passing sieve:	
No. 30	100
No. 100	97
No. 200	90
No. 325	85

TABLE 7

GENERAL CHARACTERISTICS OF POZZOLANIC BASE MATERIAL

Characteristic	AASHO Designation	Value
Composition, % by wt:		
Lime		4
Fly ash		14
Gravel		82
Max. dry den.	T99-49	135.4
Opt. moist. cont.	T99-49	7.8

Table 4. Properties of the fly ash used in the pozzolanic base are given in Table 5. Properties of the monohydrated dolomitic lime used are given in Table 6.

The general characteristics of the pozzolanic base material are given in Table 7. Figure 1 shows the general relationship between strength and age for the pozzolanic material cured under ambient conditions in the laboratory. There was a continuous strength gain of the material over an extended period of time, with the rate of gain varying somewhat for the different test sets because of differences in the ambient conditions. The trends shown in the figure are average values. Specimens cured in moist sand at approximately 70 F for 28 days attained a compressive strength of 710 psi, and those cured for 7 days in a sealed container at 130 F attained a compressive strength of 1,360 psi.

Flexural strength of the material was determined using 3- by 3- by 12-in. specimens loaded at the one-third points in accordance with the procedures outlined in ASTM Standard Test D-1360. Compressive strength specimens were the standard 4-in. diameter by 4.6-in. high proctor specimens. The modulus of elasticity was evaluated by measuring the maximum strains at the top and bottom of the flexure specimens using SR-4 strain gages bonded to the specimens. The modulus of elasticity was calculated from the curvature in the specimens as determined from the maximum strains at the top and bottom of the specimen. Poisson's ratio was determined in the usual manner, using transverse strain measurements on the compressive specimens, and was in the range of 0.08 to 0.15. A value of 0.10 was selected as an average value for routine calculations. The coefficient of thermal expansion for the material was approximately 6×10^{-6}.

The hardened pozzolanic material exhibited no weight loss during the freezing and thawing or wetting and drying durability tests. Fatigue characteristics of the pozzolanic material have been studied and the results reported (2). Because of the strength gain in characteristics of the pozzolanic material during the repeated load applications, the fatigue life of the material is highly sensitive to the age at initial loading and the rate of load applications. Thus the general fatigue characteristics can be used only as a general guide for evaluating the material's fatigue life.

The pozzolanic base materials were proportioned and mixed at approximately the optimum water content for maximum density in a 1½-cu ft pug mill mixer. The pozzolanic base was placed in the test track, leveled, and compacted with pneumatic tampers in the manner described for the compaction of the subgrade material. After compaction, the material was trimmed to the desired elevation with the planer.

Experimental Test Pavements

The test track was divided radially into 6 segments for pavement testing, each segment making a separate test pavement with either a transition section or a construction joint placed between each test pavement. A test set is composed of 6 test pavements placed and tested simultaneously in the test track. Test pavements in the various sets are given in Table 1.

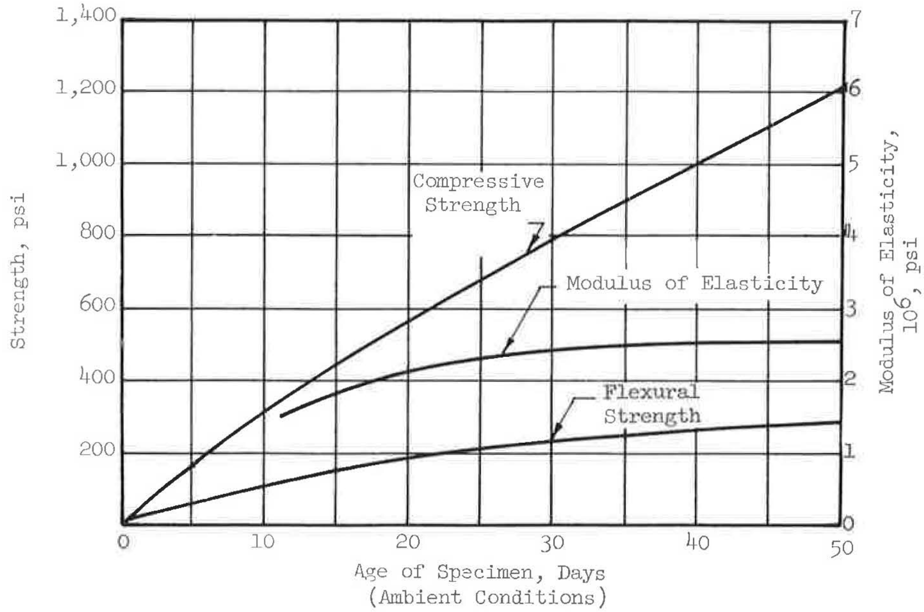

Figure 1. Strength-age relationships for pozzolanic base material.

TABLE 8

ULTIMATE CAPACITY OF STATICALLY LOADED PAVEMENTS, TEST SET I

Characteristic	Load No.							
	1	2	3	4	5	6	7	8
Load placement	Int.[a]	Int.	Int.	Int.	Edge	Edge	Int.	Int.
Age at loading, days	8	9	21	22	24	25	5	6
Flex. strength at loading, psi	98	104	275	280	290	293	79	86
Ultimate load, lb	8,750	6,000	17,750	16,250	5,750	5,750	8,250	10,000
Deflection at ultimate load, in.	0.164	0.105	0.214	0.219	0.070	0.080	0.227	0.151

[a]Int. = interior load placement.

Static Load Tests

Static tests were conducted on the pavements in test set I. The pavements were tested at different ages to study the effect of the strength of pozzolanic materials on the load deflection and ultimate load-carrying capacity of the pavements. Positions of the test loads and the age at testing are shown in Figure 2. A summary of the results from control tests on the pozzolanic material is given in Table 8. The eight test pavements were made possible because a portion of the pavement tested in the first stage was removed and replaced with a new pavement section (Fig. 2). Six pavements were tested under loads placed at an interior point on the pavement, and 2 were tested with the loading plate tangent to the edge of the pavement.

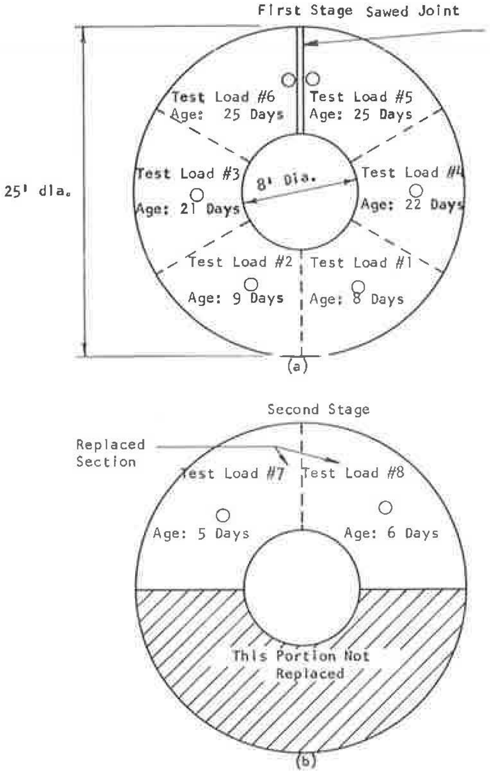

Figure 2. Plan view showing location of static test loads and age at testing.

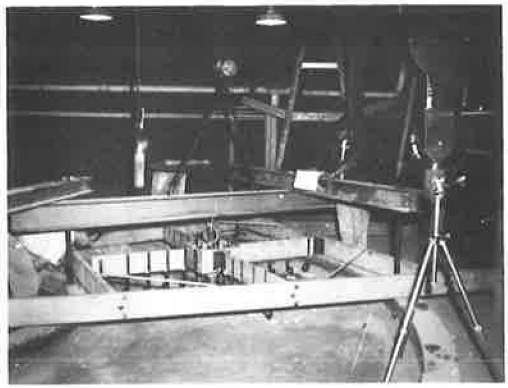

Figure 3. Overall view of reaction frame and dial indicator support frame for static load tests showing test in progress.

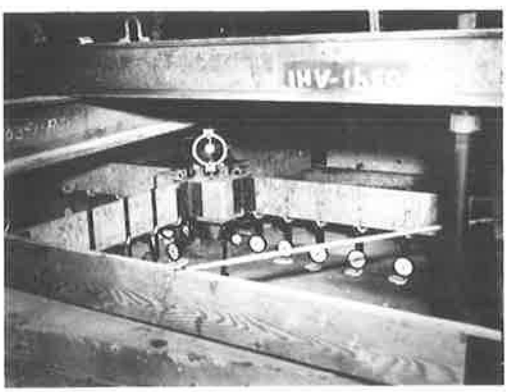

Figure 4. Closeup showing the position of the dial indicators with base of loading jack and proving ring in left center.

Static loads were applied to the test pavements by means of a hydraulic jack and a reaction frame. The loads were applied in increments which were made progressively smaller as the ultimate capacity of the pavements was approached. All loads were applied through a 7-in. diameter plate set on a quick setting mortar for easy leveling. The 7-in. plate was used because it covers approximately the same area as the tires used on the loading frame.

The deflection of the loading plate was measured by four dial indicators resting on an 18-in. diameter plate inserted between the 7-in. loading plate and the loading jack. The deflection of the pavement surface away from the loaded area was also measured with dial indicators resting on smoothed hydrocal pads cast on the pavement surface. All dial indicators were supported from a special frame supported outside the pavement test area. The reaction frame, dial indicator support frame, and the dial indicators in place are shown in Figures 3 and 4. The location of the dial indicators for the interior and edge loads are shown in Figures 5 and 6, respectively.

Load deflection curves for loads placed at the interior points on the pavement surface are shown in Figure 7. Deflection profiles for selected loads are shown in Figures 8 through 13. Theoretical deflections given by Westergaard's equations (3) are also shown in the figures. Similar curves for the edge loading condition are shown in Figures 14, 15, 16, 17 and 18. A resumé of the ultimate loads for the pavements and the strength of the pozzolanic material at the time of testing is given in Table 8.

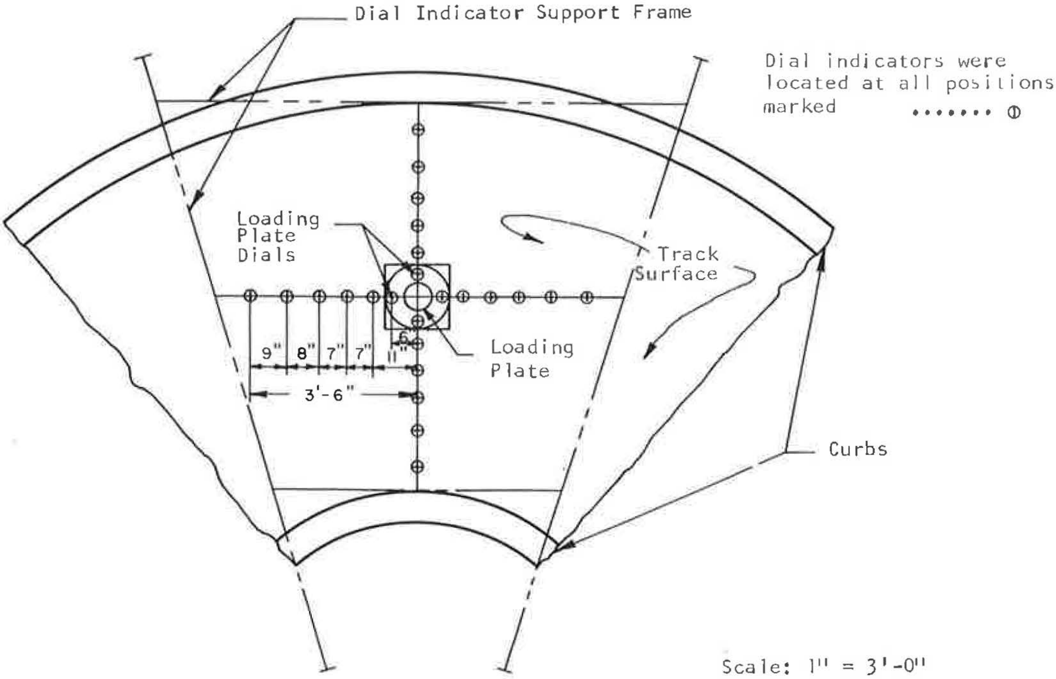

Figure 5. Plan view showing location of dial indicators for measuring surface deflection under static loads at interior point on pavement.

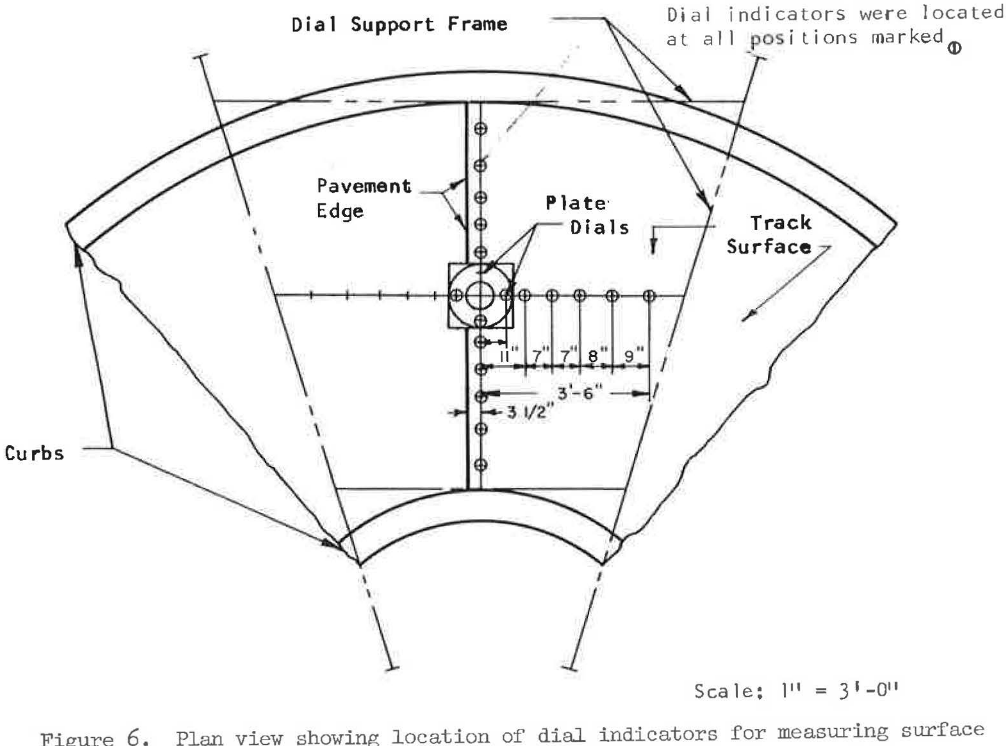

Figure 6. Plan view showing location of dial indicators for measuring surface deflection under static loads applied near edge of pavement.

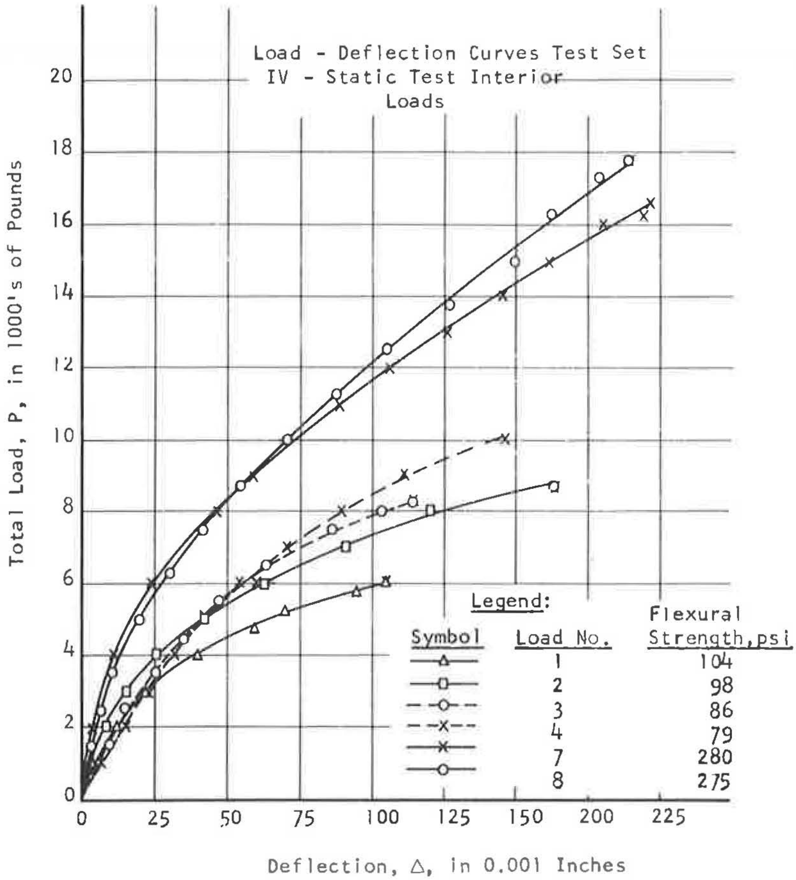

Figure 7. Load deflection curves for pozzolanic pavements under static loads at interior point.

Test pavements under interior loading failed by punching a cone from the pavement. After the pavements had failed, a section approximately 2½ ft sq was sawed from the pavement and removed, thus exposing the punched-out cone. The removed sections and the cones are shown in Figures 19 and 20. The crack patterns on the bottom surface of the cones are particularly significant.

Pavements tested under edge loads failed by developing semicircular cracks at an interior point (Figs. 21 and 22). The initial crack always appeared first along a radial line perpendicular to the pavement edge. The crack farthest from the pavement edge in Figure 21 appeared first, with the crack nearer the edge developing as additional loads were applied.

Dynamic Load Tests

The test pavements of test sets II, III and IV were tested under dynamic loads in the pavement test track. A general layout of the test track and supporting area is shown in Figure 23, and the loading frame used in the dynamic testing is shown in Figure 24. The loading frame revolves at a rate of approximately 25 rpm, and with each revolution 2 wheel loads up to approximately 3,200 lb each are applied to the pavement. The loading frame oscillates radially as it revolves allowing the loads to be applied over a wheelpath ranging from the width of the tire up to a width of approximately 30 in. (1). Test sets II and III were tested under interior loading conditions. A thickened transition section was used between the different pavement sections to provide continuity

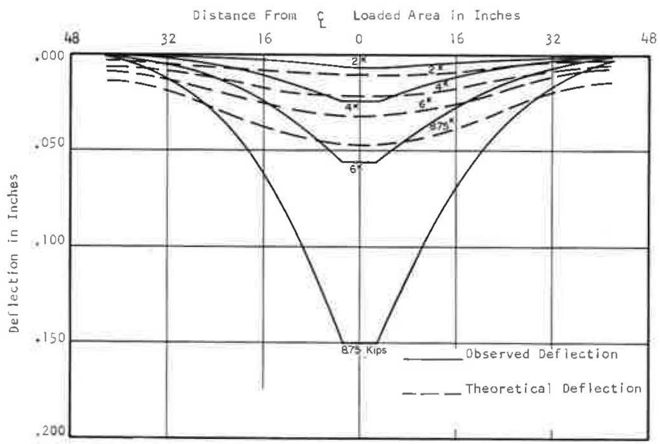

Figure 8. Load No. 1: surface deflection of pozzolanic base under static load at interior point.

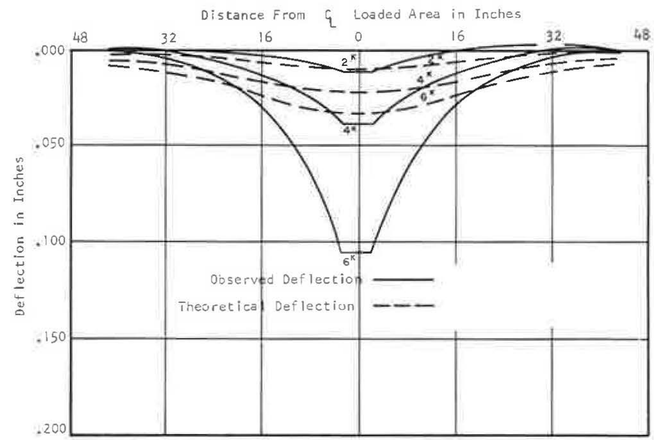

Figure 9. Load No. 2: surface deflection of pozzolanic base under static load at interior point.

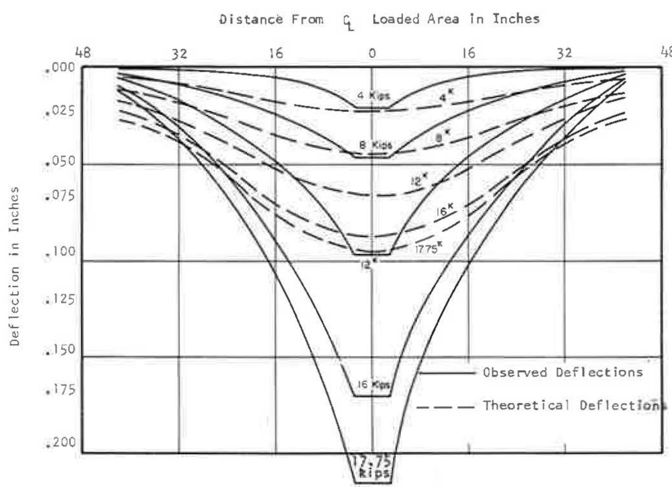

Figure 10. Load No. 3: surface deflection of pozzolanic base under static load at interior point.

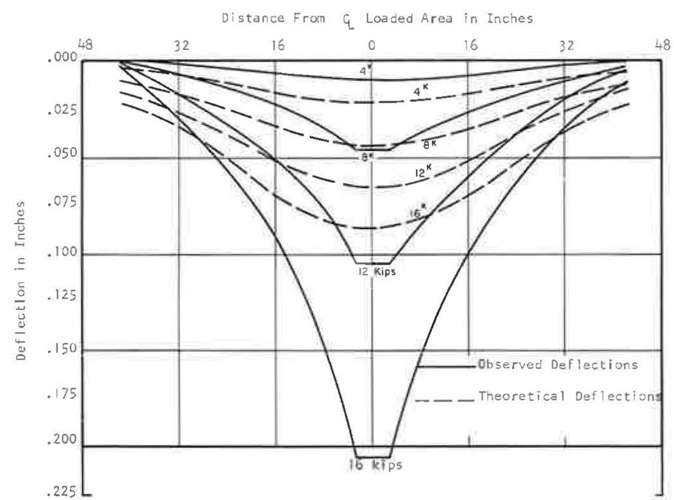

Figure 11. Load No. 4: surface deflection of pozzolanic base under static load at interior point.

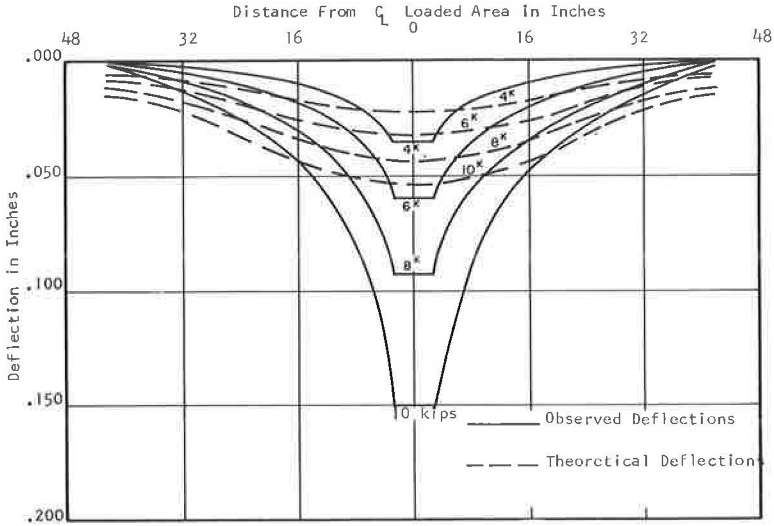

Figure 12. Load No. 7: surface deflection of pozzolanic base under static load at interior point.

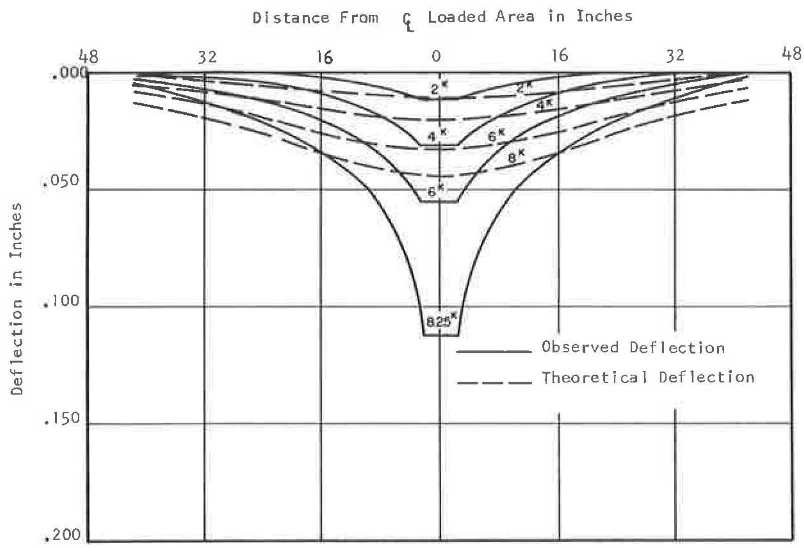

Figure 13. Load No. 8: surface deflection of pozzolanic base under static load at interior point.

of pavement action between test pavements. Test set IV was constructed to test the behavior of pavements under edge loading conditions. Construction joints, which provided no load transfer between pavements, were placed between the pavements thus simulating the most severe edge loading condition anticipated from a transverse crack across a pavement.

Initial loading was applied to the test pavements of test set II after accelerated curing equal to approximately 28 days under ambient conditions. At the time of initial loading, the pozzolanic-stabilized material had a modulus of rupture of 185 psi. A summary of the properties of the pozzolanic material and the gain in strength during loading is given in Table 9. More than a million applications of the 1, 850-lb wheel load were applied to the test pavements of test set I during the 120-day period. After

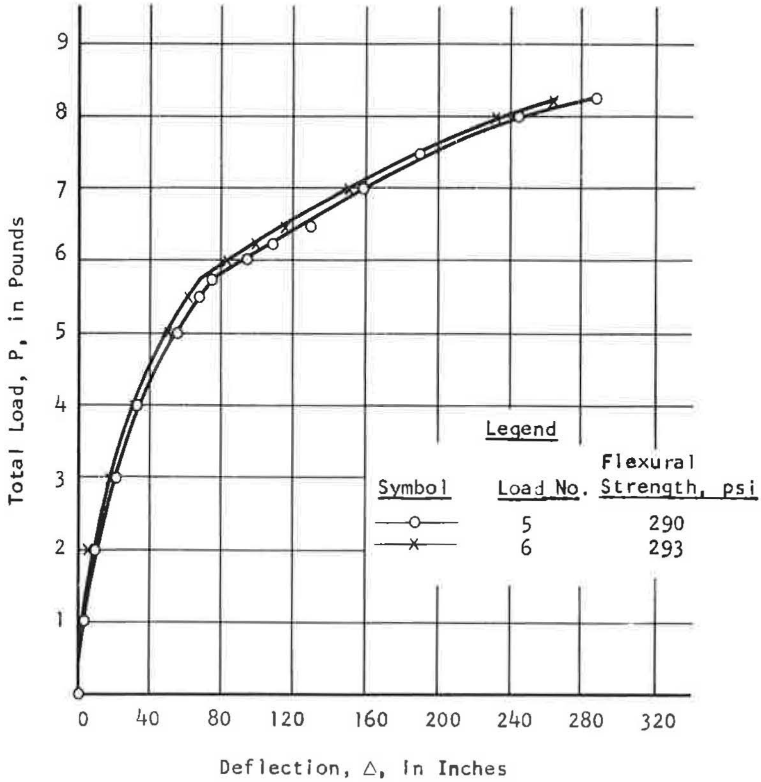

Figure 14. Load Deflection curves for static loads 5 and 6, applied near edge of pavement.

the million loads had been applied without evident distress in the pavements, the load was increased to 3,180 lb/wheel and an additional 300,000 load applications applied. Again, there was no sign of pavement distress, and since the strength of the material was increasing continuously further testing was terminated. Flexural strength of the pozzolanic material at the termination of the test was well in excess of 350 psi.

Pavements in test set III were loaded initially with the 3,180-lb wheel load 5 days after placement of the pozzolanic-stabilized material. Again, the pavements were tested under interior loading conditions with the thickened transition section between pavements. The thickness of the test pavements is given in Table 1, and a summary of the strength and strength gain properties for the pozzolanic material for test set III is given in Table 10.

Slightly more than 500,000 load applications were applied to test pavements of test set III in a 14-day period. During this time the modulus of rupture of the pozzolanic material increased from approximately 75 psi to 192 psi. Test pavements 1 and 5 failed during the first day of loading operation with a well developed crack pattern readily apparent after approximately 15,000 load applications. There is some indication that the initial failure of test pavements occurred after approximately 5,000 load applications but the cracks on the surface were not readily apparent at that time. A map of the crack pattern from the surface of test pavement 1 is shown in Figure 25. A section taken across the wheelpath of test pavement 1 after failure is shown in Figure 26.

Test pavement 5 of test set III deteriorated so rapidly, and to such an extent, that the crack development and the failure pattern could not be studied. After complete failure of test pavement 5, the pozzolanic material was removed with honeycombing and segregation of the aggregate observed near the bottom of the test pavement.

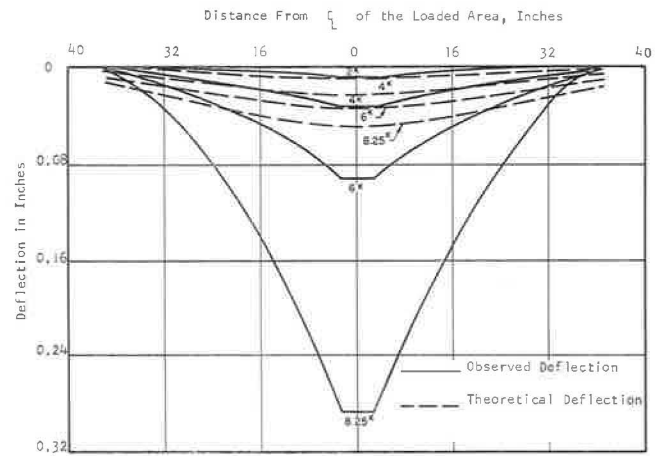

Figure 15. Load No. 5: surface deflection of pozzolanic pavement parallel to edge of pavement under static loads applied near edge.

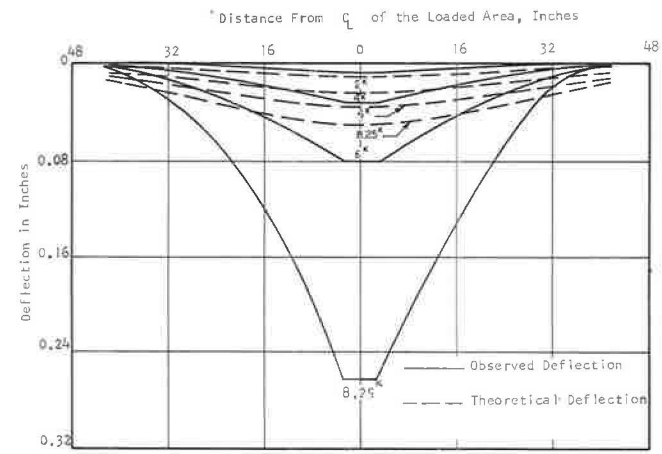

Figure 16. Load No. 6: surface deflection of pozzolanic pavement parallel to edge of pavement under static loads applied near edge.

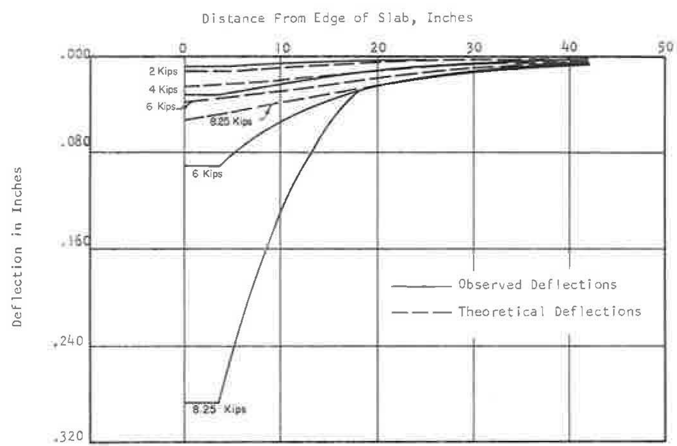

Figure 17. Load No. 5: surface deflection of pozzolanic pavement along line perpendicular to edge of pavement, under static load applied near edge.

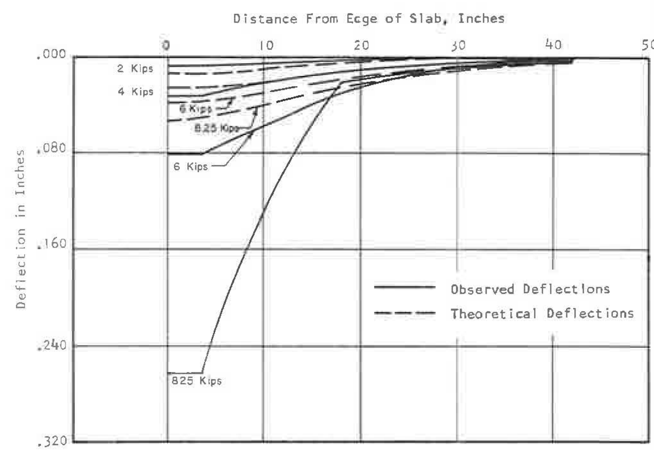

Figure 18. Load No. 6: surface deflection of pozzolanic pavement along line perpendicular to edge of pavement, under static load applied near edge.

Application of the loads on pavements 2, 3, 4 and 6 was terminated after the 500, 000 applications as it was evidenct that no further pavement distress was occurring, and the strength of the pozzolanic material had increased to such an extent that pavement damage due to repeated load applications was unlikely.

Test set IV was designed to evaluate pozzolanic pavements under edge load conditions with dynamic loads. Two pavement thicknesses of 4. 0 and 5. 5 in. were tested with one test pavement of each thickness placed on each of 3 different days so that the effect of both thickness and strength on the ability of the pavement to withstand repeated load applications could be evaluated. Pavement thickness, age at the start of testing, properties of the subgrade, and properties of the pozzolanic stabilized material for test set IV are given in Table 11. Edge conditions for the test pavement were obtained by forming construction joints at the intersection of the test pavement sections. These construction joints were filled with an asphaltic patching mixture before testing.

Test pavement 1 showed excessive deflection with the first load application, and after approximately 10 load applications a network of cracks was clearly visible on the pavement surface. After approximately 40 load applications, the pavement had disintegrated to the extent shown in Figure 27.

Visible cracks appeared on the surface of test pavement 6 after approximately 80 load applications. The cracks expanded with additional load applications and additional cracks developed. After approximately 140 load applications, cracks were also visible in test pavement 2. After approximately 175 load applications, the crack patterns in test pavements 2 and 6 had developed to the extent shown in Figures 28 and 29. Complete structural failure followed the initial cracking of both test pavements 2 and 6. Test pavement 2 had failed completely after approximately 600 load applications and test pavement 6 after approximately 1, 700 load applications, all of which were applied during the first day of loading. After failure, test pavements 1, 2 and 6 were replaced with a high early strength concrete pavement so that additional load applications could be applied to the remaining test pavements.

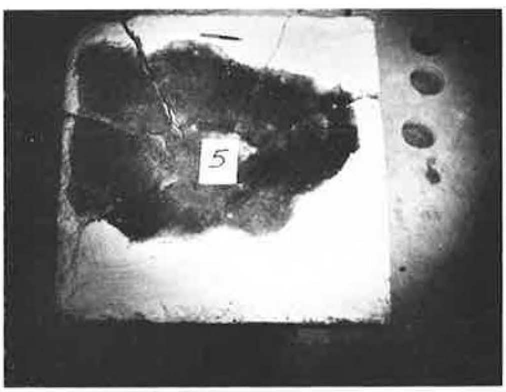

Figure 19. Bottom face of inverted section of pavement after failure under static load.

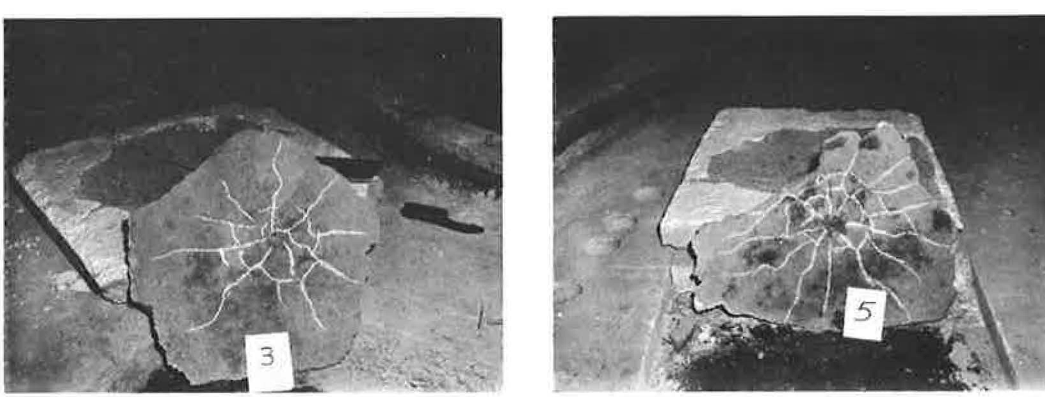

Figure 20. Bottom surface of typical cones punched out of pavement in static load tests.

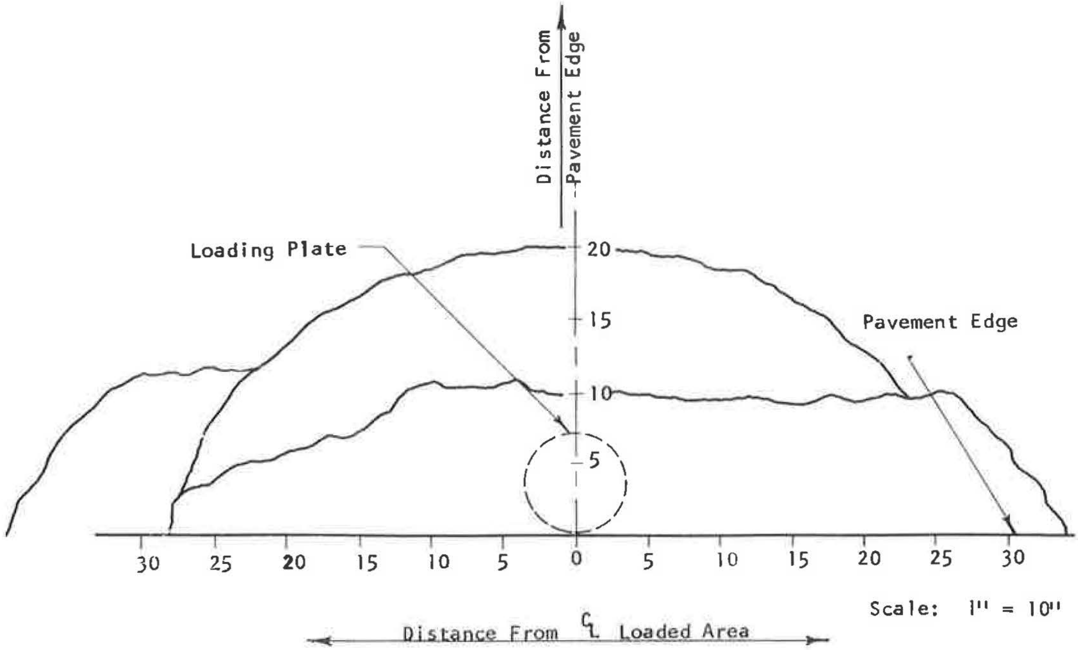

Figure 21. Load No. 5: crack pattern on surface of pavement at end of static load test.

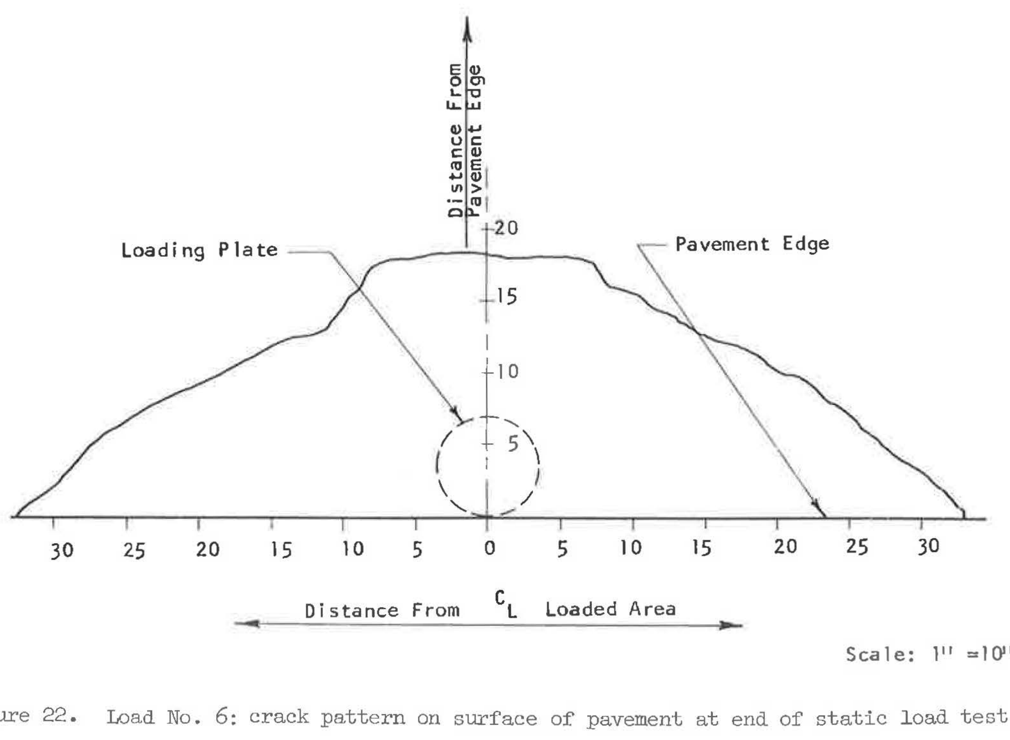

Figure 22. Load No. 6: crack pattern on surface of pavement at end of static load test.

TABLE 9

SUMMARY OF DATA ON POZZOLANIC MATERIAL FOR PAVEMENT OF TEST SET II

Strength Property	Age[a] (days)					
	0	4	12	28	50	120
Flexural, psi	185	196	219	254	257	352
Compressive, psi	1,110	1,140	1,080		1,520	1,680
Modulus of elasticity, $\times 10^6$, psi[b]		2.3	2.5	2.3	2.4	2.5

[a]After initial loading.
[b]The modulus of elasticity was determined from strain measurements on flexure specimens.

TABLE 10

SUMMARY OF DATA ON POZZOLANIC STABILIZED MATERIAL FOR TEST PAVEMENT OF TEST SET III

Strength Property	Age[a] (days)		
	0	5	14
Flexural, psi	75	160	192
Compressive, psi	420	890	1,180
Modulus of elasticity, $\times 10^6$, psi	1.3	1.9	—

[a]After initial loading.

TABLE 11

SUMMARY OF DATA ON POZZOLANIC MATERIAL FOR TEST PAVEMENT OF TEST SET IV

Strength Property	Age[a] (days)					
	5	9	16	16	9	5
Flexural, psi	76	170	230	230	170	76
Compressive, psi	300	580	800	800	580	300

[a]After initial loading.

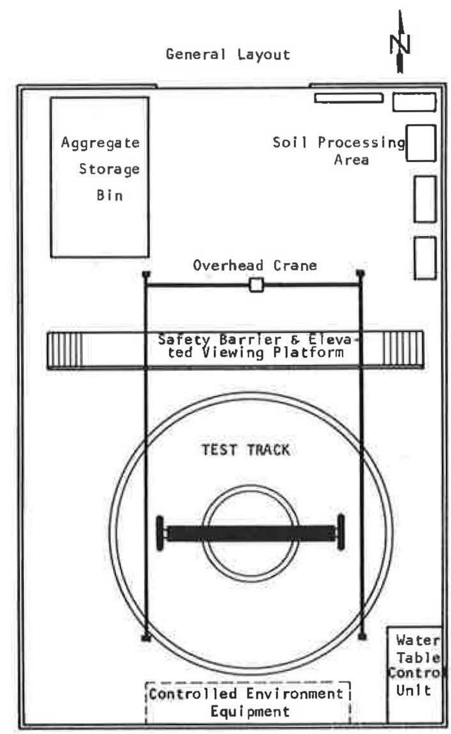

Figure 23. University of Illinois pavement test track.

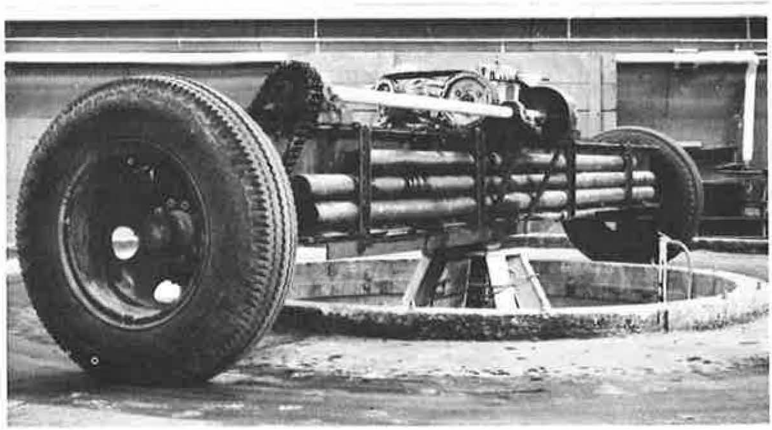

Figure 24. Loading frame used in test track for dynamic load tests.

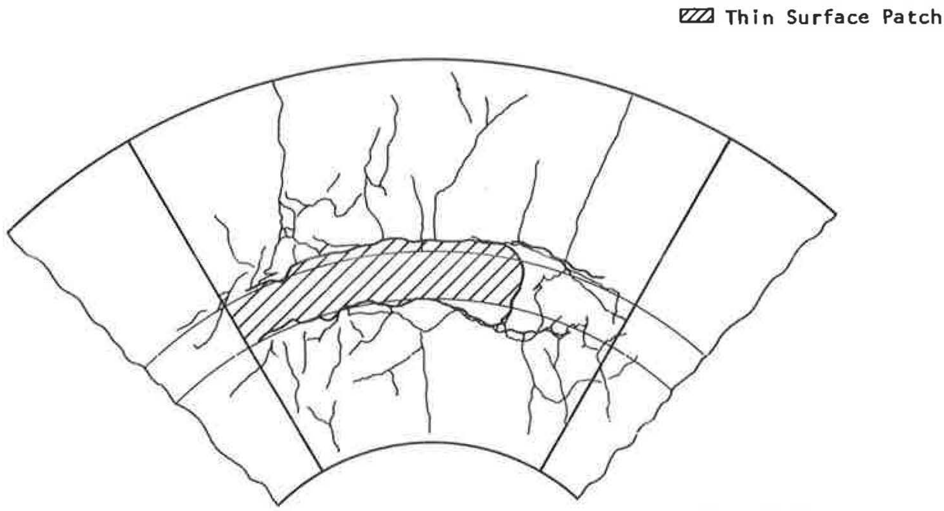

Figure 25. Surface crack pattern of test pavement 1, test set III, after approximately 15,000 load applications.

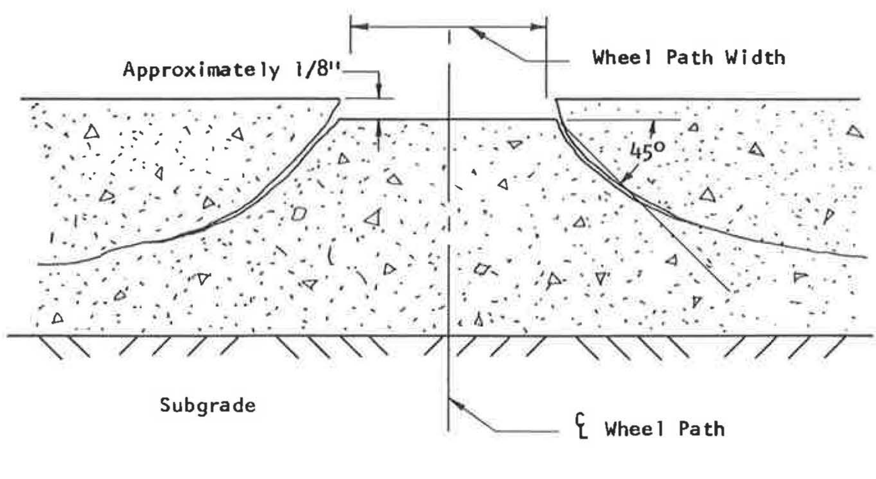

Figure 26. Test pavement 1, test set III: section through wheelpath in area of failure after approximately 15,000 load applications.

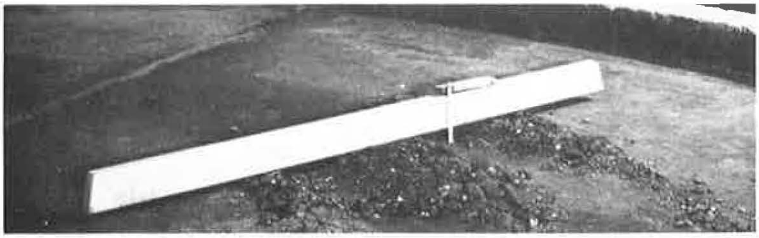

Figure 27. Test pavement 1 of test set IV after 40 applications of load, showing severe rutting and complete disintegration of material caused by excessive load applied before adequate curing.

Figure 28. Crack patterns observed on test pavement 2 of test set IV after 175 load applications with white paint applied to outline location of cracks.

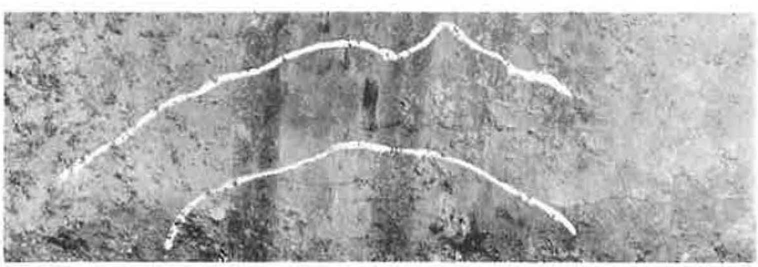

Figure 29. Crack patterns observed on test pavement 6 after 175 load applications,with white paint applied to outline location of cracks.

Testing resumed on the remaining test pavements approximately 36 hr after the initial loading, and slightly more than 500, 000 applications of the 3, 180-lb wheel load were applied to test pavements 3, 4 and 5 without any evidence of pavement distress. At this time, the loading was discontinuous because the apparent gain in strength of the material had made pavement failure under repeated load applications unlikely.

RESULTS

Pozzolanic stabilized materials take on additional set with time and become hard and resistant to flexing. Pavements made of these materials, after a reasonable set, distribute the load over an extended area of subgrade in the same manner as plain concrete pavements, and thus should be classified as rigid pavements. The extent of the load distribution is evident in the results from the static load tests.

Elastic theories of pavement behavior such as Westergaard's (3) equations accurately predicted the deflection profile and the maximum deflection of the pozzolanic pavements under static loads, provided the load was significantly less than the ultimate load carrying of the slab. As the load was increased above approximately one-half the ultimate load-carrying capacity of the slab, the pavement deflection increased more than indicated by the elastic theory with each load increment. These elastic theories of pavement behavior were, however, completely invalid for predicting the ultimate load-carrying capacity of the slab, as the latter was many times greater than that indicated by the elastic theories and the modulus of rupture for the material.

Meyerhof (4) developed equations for estimating the ultimate load-carrying capacity of plain concrete slabs based on the Rankine failure criterion for the material. Since the physical properties of hardened pozzolanic materials are similar to those of plain concrete, Meyerhof's equations should also apply to the pozzolanic material.

According to Meyerhof, the failure of nonreinforced slabs made from a material much stronger in compression than in tension should proceed in the following manner. When a central concentrated load, much less than ultimate, is applied over a small circular area on a slab in full contact with the base, the stresses and deflection of the slab can be computed using elastic theories for infinite slabs on an elastic subgrade. As the load increases, the bending stresses below the load become equal to the flexural strength of the material and the slab begins to yield, leading to radial tensile cracks in the bottom of the slab (Fig. 30a). With increasing load the radial cracks increase in length until the circumferential, flexural stresses along the arc with radius b become equal to the flexural strength of the material, at which time a circumferential crack appears on the slab surface and the slab collapses completely. The initial yield moment along a unit section of the slab can be calculated from elastic theory, with the yield moment of the slab given by

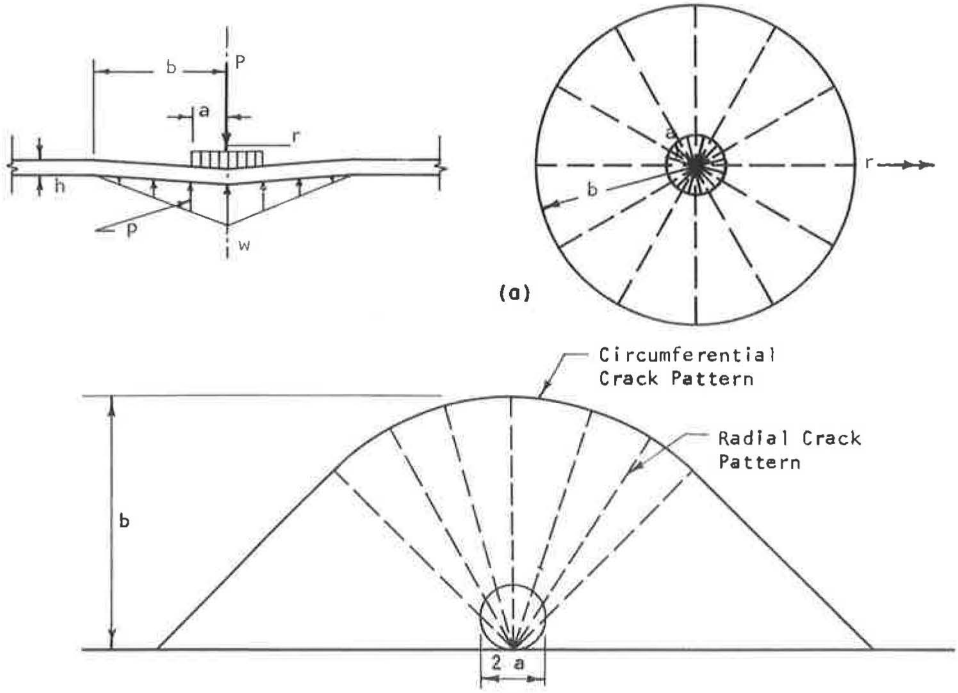

Figure 30. Failure pattern of rigid slab under (a) interior loading and (b) edge loading, as predicted by Meyerhof (4).

$$M_y = \frac{f_b h^2}{6} \tag{1}$$

where

M_y = yield moment per unit length of slab,
h = slab thickness, and
f_b = modulus of rupture of the material.

Using the dense liquid subgrade assumed by Westergaard, the radius of relative stiffness for the pavement is given by

$$L = \sqrt[4]{\frac{E h^3}{12(1 - \mu^2)k}} \tag{2}$$

where

E = modulus of elasticity of the slab,
k = modulus of subgrade reaction, and
μ = Poisson's ratio.

With this nomenclature, Meyerhof showed that the ultimate load-carrying capacity of the slab under interior loads is given by

$$P_o = \frac{4\pi M_o}{\left(1 - \frac{a}{3L}\right)} \quad \left(\text{for } \frac{a}{L} > 0.2\right) \tag{3}$$

where

M_o = yield moment for the slab, and
a = radius of the circular loaded area.

For a concentrated load applied over a circular area placed tangent to the edge of the slab, the yield load can again be estimated from elastic theory. As the load increases beyond that causing yield stresses in the bottom of the slab, radial tension cracks develop and widen until a circumferential crack (Fig. 30b) forms on the surface leading to the complete collapse of the slab. The collapse load for plain concrete slabs under edge loads is given by

$$P_o = \frac{(\pi + 4) M_o}{\left(1 - \frac{2a}{3L}\right)} \quad \left(\text{for } \frac{a}{L} > 0.2\right) \tag{4}$$

The limit of $a/L > 0.2$ in Eqs. 3 and 4 is based on the assumption that the circumferential crack is at a distance of 3L from the loaded area. Since the crack usually forms at a distance of 2L or less from the load, this ratio can be reduced somewhat.

Since, for nonreinforced slabs, $M_o = M_y = (f_b h^2)/6$, Eqs. 3 and 4 can be rewritten in the following forms:

For interior loads:

$$P_o = \frac{2\pi f_b h^2}{3\left(1 - \frac{a}{3L}\right)} \tag{5}$$

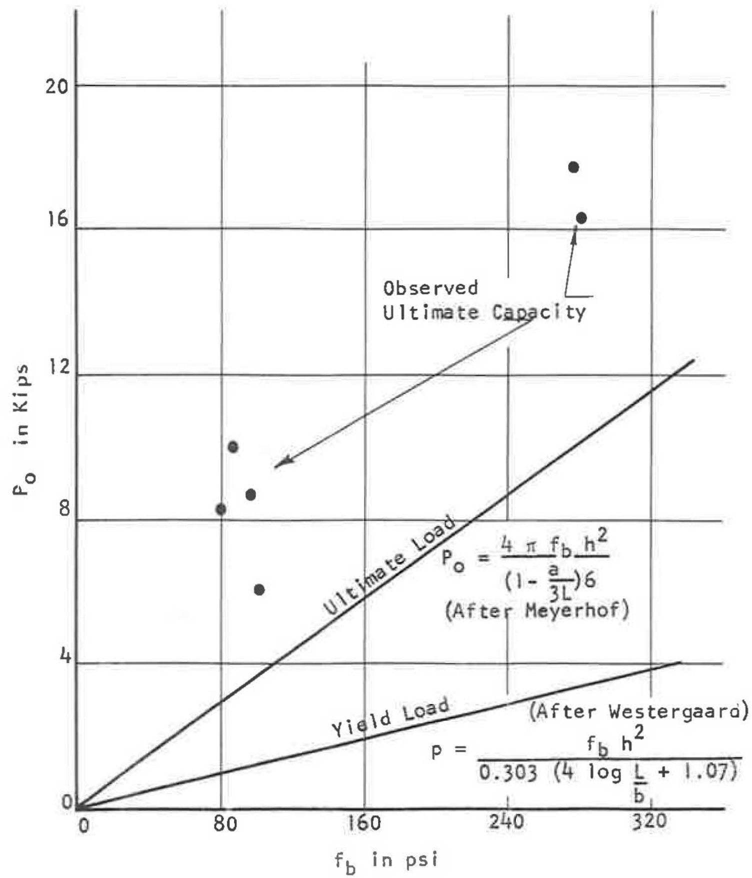

Figure 31. Comparison of theoretical failure loads and observed ultimate loads for 4 in. pozzolanic pavement under interior loading.

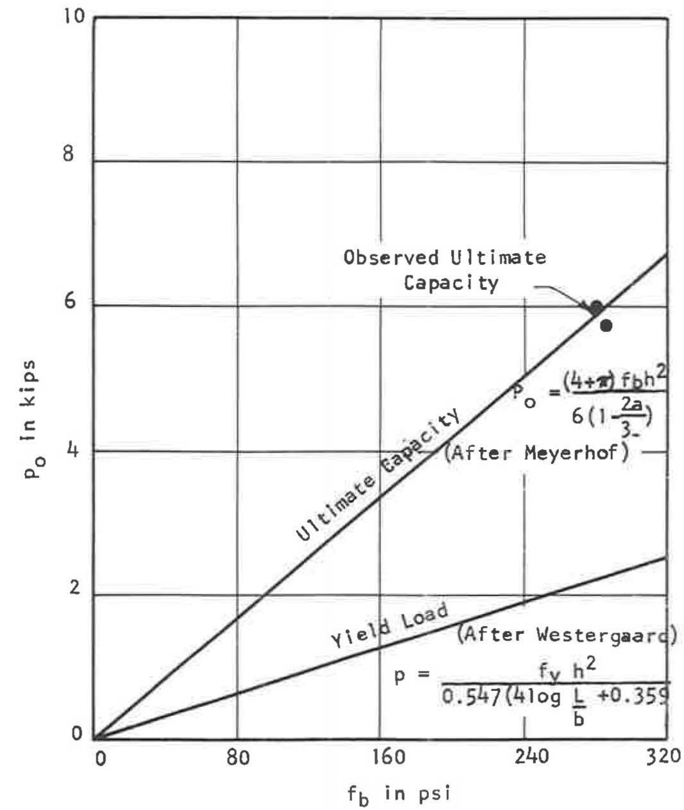

Figure 32. Comparison of theoretical failure loads and observed ultimate loads for 4 in. pozzolanic pavement under edge loading.

For edge loads:

$$P_o = \frac{(4+\pi)\, f_b\, h^2}{6\left(1 - \frac{2a}{3L}\right)} \tag{6}$$

Comparison of the theoretical ultimate loads given by Eq. 5 and the results from the interior load test are shown in Figure 31. Comparison of the ultimate load given by Eq. 4 and the results from the edge load tests are shown in Figure 32. The yield loads determined from Westergaard's equations are also shown on the appropriate figures.

The theoretical collapse load given by Meyerhof's theory is approximately 2.5 to 3 times the yield load for the slabs. Since the elastic theory was valid for all loads of less than one-half of ultimate, the deflection predicted by the elastic theory could be assumed valid for loads up to the yield load for the pavement.

Failure under the interior loads was a pop-through type failure and the anticipated circumferential crack on the pavement surface did not develop. However, the ultimate load at failure for all interior loads was greater than predicted by Meyerhof's theory. A possible explanation for this behavior is the arching action which develops in large slabs made of a material much stronger in compression than in tension. As yielding occurs in the areas of high tensile stress, there is a concomitant shift in the neutral axis of the slab. This shifting of the neutral axis causes the arching action (Fig. 33),

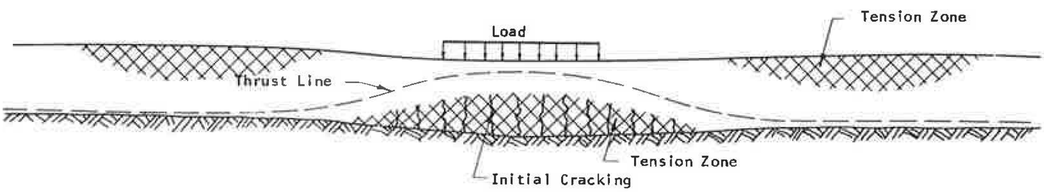

Figure 33. Schematic of stress pattern and arching phenomenon in slabs loaded at interior point.

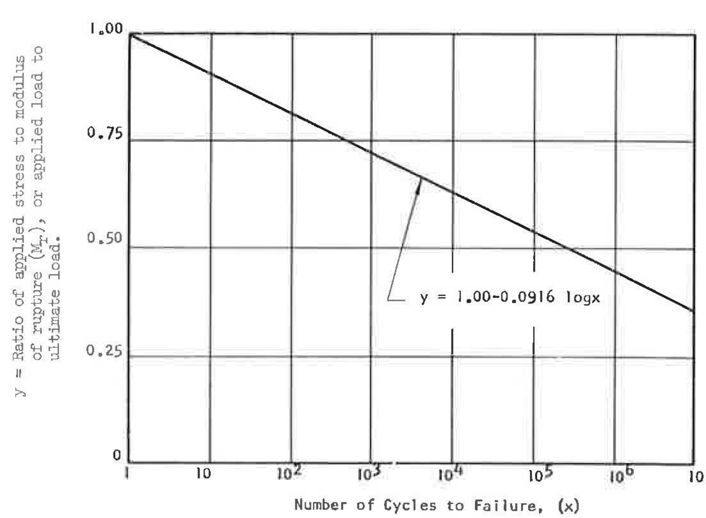

Figure 34. Fatigue behavior of lime-fly ash-aggregate-mixture (2).

which in turn prevents the circumferential crack from developing as expected. Radial cracks developed in the bottom of the slab as expected (Fig. 20).

Arching action does not develop near the edge of the pavement and, as a result, the failure mechanism under the edge loads was more nearly as anticipated. The observed collapse load under the edge loading is in good agreement with the values given by Meyerhof's equations.

Test sets II, III and IV were tested under repeated dynamic loads and thus should be analyzed in terms of the fatigue properties of the material. Fatigue properties of the pozzolanic material used in the test pavements were reported by Ahlberg and McVinnie (2), and the results are summarized in Figure 34.

The classical method for evaluating the fatigue properties of materials is to determine the number of load applications to failure based on a ratio of the stress in the slab to the modulus of rupture of the material. However, the results of the fatigue tests can also be interpreted in terms of the ultimate strength criterion. Since the modulus of rupture for the fatigue specimens is calculated from the ultimate load applied to the specimen and based on the linear theory, there is a linear relationship between the modulus of rupture and the ultimate load the specimens can carry. Therefore, since the number of load applications to failure determined from the ratio of the applied to the ultimate collapse load is the same as for the ratio of the theoretical to the failure stress, the load ratio criterion can also be used to evaluate the fatigue life of the pavements. A comparison of the expected number of load applications to failure, using the ratio of theoretical stress to yield stress and the ratio of applied load to ultimate load for test sets II, III and IV, is given in Table 12.

Neither the stress ratio criterion nor the load ratio criterion accurately predicted the number of load applications to failure for the interior loads of test sets II and III, although the load ratio criterion gave a better indication of the potential load carrying capacity than the stress ratio criterion. With both criteria the actual performance of

TABLE 12

SUMMARY OF RESULTS FROM DYNAMIC TESTING PROGRAM

Pavement No.	Pavement Thickness (in.)	M_r at Init. Loading (psi)	Applied Load	Theoret. Stress by Elastic Theory (psi)[a]	Ult. Load-Carrying Cap. (lb)[b]	Ratio of Theoret. Stress to M_r	Ratio of Applied Load to Ult. Load	Expected Load Applications to Failure[c]		Loads Applied to 1st Observed Failure[d]
								Using Theoret. Stress to M_r Ratio	Using Applied to Load Ratio	
					Test Set II					
1	4.3	185	1,850	122	8,200	0.66	0.23	5,100	1×10^8+	1×10^6+[e]
3	3.8	185	1,850	150	6,000	0.81	0.31	120	7×10^7-	1×10^6+
4	4.8	185	1,850	101	9,500	0.55	0.20	81,000	1×10^8+	1×10^6+
5	4.3	185	1,850	122	8,200	0.66	0.23	5,100	1×10^8+	1×10^6+
					Test Set II					
1	4.3	260	3,180	210	11,500	0.81	0.28	120	1×10^8	3×10^5[e]
3	3.8	260	3,180	258	8,400	0.99	0.28	1	1×10^7	3×10^5+
4	4.8	260	3,180	174	13,300	0.67	0.24	4,000	1×10^8+	3×10^5+
5	4.3	260	3,180	210	11,500	0.81	0.28	120	1×10^8	3×10^5+
					Test Set III					
1	4.3	75	3,180	198	3,120	>>1	1.02	<<1	1	1.5×10^4
2	4.8	75	3,180	168	3,880	>>1	0.82	<<1	90	5×10^5+
3	5.3	75	3,180	143	4,680	>>1	0.68	<<1	3,100	5×10^5+
4	5.8	75	3,180	122	5,620	>>1	0.56	<<1	63,000	5×10^5+
5	4.8	75	3,180	168	3,880	>>1	0.82	<<1	90	1.5×10^4
6	5.3	75	3,180	143	4,680	>>1	0.68	<<1	3,100	5×10^5+
					Test Set IV					
1	4.0	76	3,180	360	1,630	>>1	1.95	<<1	<1	<10
2	4.0	170	3,180	385	3,650	>>1	0.87	<<1	20	175
3	4.0	230	3,180	395	4,880	>1	0.65	<1	7,000	5×10^5+
4	5.5	230	3,180	230	9,050	1.00	0.35	1.0	1×10^7	5×10^5+
5	5.5	170	3,180	227	6,230	>1	0.51	<1	3×10^5	5×10^5+
6	5.5	76	3,180	213	3,030	>>1	1.05	<<1	$\simeq 1$	80

[a]Data derived from reference 3.
[b]Data derived from reference 4.
[c]Data derived from Figure 34.
[d]Values with + sign showed no sign of failure at termination of the loading program.
[e]Pavements loaded with 1 million applications of the 1,850-lb. load followed by 300,000 applications of the 3,180-lb. load.

TABLE 13

EFFECT OF STRENGTH GAIN WITH AGE ON THE NUMBER OF LOADS
(Test Pavement 3, Test Set IV)

Characteristic	Age[a] (days)				
	0	1 1/2	3	10	16[b]
Flexural strength, psi	230	247	260	310	340
Ult. load-carrying capacity	4,880	5,250	5,520	6,600	7,240
Applied load	3,180	3,180	3,180	3,180	3,180
Load ratio	0.65	0.61	0.58	0.48	0.44
No. of loads to failure based on load ratio at age indicated	7×10^3	1.6×10^4	3×10^4	4×10^5	8×10^5
Cumulative loads applied through day indicated	1.7×10^3	8×10^3	3×10^4	2×10^5	5×10^5

[a]After initial loading.
[b]Testing stopped at 500,000 load applications on this day.

the pavements far exceeded the expected performance. There are several possible reasons for this phenomenon.

As shown in Figure 31, the actual load-carrying capacity of the pavements under interior loads is somewhat greater than predicted by the ultimate theory, thus giving an actual load ratio less than that assumed from theoretical calculations. This decreased load ratio would lead to a higher number of load applications than indicated in the table for failure, bringing the observed load applications into better agreement with the theoretical number.

Under transient loads the supporting capacity of the subgrade is greater than indicated from static load tests. The increased subgrade support would increase the load-carrying capacity of the pavements and also give a smaller load ratio and a greater number of expected load applications to failure.

The increase in strength of the pozzolanic material during the load applications has a demonstrated effect on the number of load applications to failure (2). The potential influence of this gain in strength is demonstrated in Table 13 for test pavement 3 of test set IV. During the early part of the test the load applications accumulated faster than the increase in the required number of loads to failure, and the two were of the same order of magnitude during the third day of loading. After the third day, however, the required number of load applications to failure increased faster than the load applications could be accumulated. Since the pavement did not fail on the third day when the applied loads were equal to the number theoretically required for failure, it appeared likely that the pavement would not fail under the repeated load, and testing was terminated.

A study of the fatigue life for the pavements in test set IV indicates that the load ratio criterion is reasonably valid for predicting the expected life for the pavement of the test pavements under the edge loading. Of the pavements which did not fail, only test pavement 3 could have reasonably been expected to fail under repeated load applications when the load ratio criterion is applied. As demonstrated previously, this pavement did not fail, primarily because the gain in strength for the material was such that the pavement strength increased at a faster rate than the cumulative damage was done to the pavement. Hence, using the fatigue behavior of the material and the load ratio criterion, the failure of test pavements 5 and 6 was accurately predicted. There appears to be a consistent tendency for this procedure to give answers on the conservative side, even when using the load ratio criterion.

SUMMARY AND CONCLUSIONS

Pozzolanic materials gain strength at a relatively slow rate, but continue to gain in strength indefinitely but at a decreasing rate. Although the 7- and 28-day strengths are relatively low compared to concrete, after an extended period of time the strength of a high quality pozzolanic material may approach that of average quality concrete.

Even partially cured and hardened pozzolanic materials are stiff and resistant to flexural deformation. Measured values of the modulus of elasticity in flexure are between 1.5×10^6 and 2.5×10^6 after curing approximately 7 days under ambient conditions. With a modulus of this magnitude it can be expected that pozzolanic pavements will distribute the load over large areas of subgrade, thus producing low subgrade stresses.

Results from the pavement behavior studies clearly show that pozzolanic pavements act as slabs and distribute the load extensively, especially if the applied load is small compared with the ultimate capacity of the pavement. The load deflection characteristics of pozzolanic pavements can be predicted with reasonable accuracy with elastic theories of pavement behavior provided the calculated maximum stress in the pavement using the elastic theory is less than the modulus of rupture of the material.

The ultimate load-carrying capacity of the pavement is from two and one-half to three times the load which produces a theoretical maximum stress equal to the modulus of rupture of the material. The ultimate load-carrying capacity can be estimated by Meyerhof's theory for the collapse load.

Predicted fatigue life of pozzolanic pavements based on the yield load for the pavements is completely unrealistic. Predicted fatigue life based on a ratio of the applied to the ultimate load gives somewhat better results provided the gain in strength during the load applications is taken into account. Even with the load ratio criterion, however, the predicted life is conservative.

Based on the results from the repeated load applications on test pavements, it appears that the pozzolanic pavements which do not fail during the first several days of loading will probably not fail due to repeated load applications acting alone.

Finally, the load-carrying capacity of pozzolanic pavements can be improved either by increasing pavement thickness or by increasing the strength of the material. The simplest method for increasing the strength of the pozzolanic material is to allow additional curing time before loading. Since the rate of strength gain of pozzolanic materials is susceptible to the surrounding climatic conditions, the length of time for curing will also depend on the existing climatic factors of temperature and moisture. Sufficient curing time should be allowed before loading so that the pavement can carry the maximum anticipated load applied near the edge of the pavement without exceeding the ultimate load-carrying capacity of the pavement, with a reasonable factor of safety included.

ACKNOWLEDGMENTS

This research was carried out as a cooperative program between the University of Illinois Engineering Experiment Station and individual organizations from private industry. The author wishes to thank all those who contributed to the program.

REFERENCES

1. Ahlberg, H. L. and Barenberg, E. J. The University of Illinois Pavement Test Track — A Tool for Evaluating Highway Pavements. Highway Research Record No. 13, p. 1, 1963.
2. Ahlberg, H. L. and McVinnie, W. W. Fatigue Behavior of a Lime-Fly Ash-Aggregate Mixture. Highway Research Board Bull. 335, p. 1, 1962.
3. Westergaard, H. M. Stresses in Concrete Pavements Computed by Theoretical Analysis. Public Roads, Vol. 7, No. 2, 1926.
4. Meyerhof, G. G. Load-Carrying Capacity of Concrete Pavements. Journal, ASCE, Vol. 88, No. SM3, p. 89, June 1962.
5. The AASHO Road Test Report 2, Materials and Construction. Highway Research Board Spec. Rept. 61B, 1962.
6. The AASHO Road Test Report 5, Pavement Research. Highway Research Board Spec. Rept. 61E, 1962.